

Double-Cage Induction Motors Behavior Under Flicker Conditions

Morteza Ghaseminezhad*, Aref Doroudi† and Seyed Hossein Hosseinian‡

Voltage fluctuation (Flicker) is caused by random variations in active and reactive power drawn by loads such as electric arc furnaces. The voltage fluctuations can generate many undesirable effects on both industrial and domestic apparatus. The main purpose of this paper is to analyze the performance of a double cage induction motor under voltage fluctuations conditions. To achieve this goal several simulations were performed using small signal model of a double-cage induction motor. Current and speed changes in different levels are obtained from the voltage fluctuations and flicker frequencies. Current and speed changes of motor in different levels of the voltage fluctuations are obtained from small signal analysis. PSCAD/EMTDC tool will be applied to verify the results of the model. A quantitative approach which uses eigenvalues of motor state matrix and participation matrix is also presented.

Keywords: Flicker, Double-Cage Induction Motors, Small Signal Analysis, Voltage Fluctuations.

Received October 2012; Revised June 2013; Accepted August 2013.

I INTRODUCTION

Sensitive loads require high quality power supply. Amongst many power quality problems, voltage fluctuations (flicker) have gained a growing concern from utilities and consumers. It is reported that voltage fluctuations of less than 0.5% in the frequency range of 5-10 Hz can cause visible lamp voltage flicker [1].

The flicker is defined as “*impression of unsteadiness of visual sensation induced by a light stimulus whose luminance or spectral distribution fluctuates with time*” [1–3]. Flicker is simply an amplitude modulated signal which is usually expressed as a percent of the total change in voltage with respect to the average voltage over a specified time interval. The corresponding instantaneous voltage can be expressed as:

$$v(t) = V_p \left[1 + \sum_m \sin(2\pi f_m t + \varphi_m) \right] \cos(2\pi f_b t) \quad (1)$$

Flicker frequencies in the range of 0.05 to 35Hz can cause perceptible flicker [4]. The human eye is more sensitive to the flicker frequencies around 8.8hz [5]. Loads such as arc furnaces, rolling mills, welding machines which exhibit continuous and rapid variations in their current can cause voltage fluctuations. An example of low voltage loads that may produce voltage fluctuations, are copying machines, X-ray equipment, drives for lifts, pumps, fans, refrigerators and electric cookers [1]. In certain conditions, superimposed inter harmonics in the supply voltage can lead to oscillating luminous flux. Sources of inter harmonics include static frequency converters, sub-synchronous converter, induction machines and arc furnaces [1, 6].

Due to load characteristics, the flicker behavior can be cyclic,

chaotic and stochastic. However; in a short period the voltage flicker can be approached by an amplitude modulated formula (1) [5]. Voltage flicker reduces the lifetime degradation of the electronic, incandescent and fluorescent lights performance. It has been also observed that the voltage fluctuations may cause small speed changes in electrical motors which lead to variations in final quality of products [1, 2]. The voltage flicker sources and mitigation methods can be found in [7].

However, being the induction motor is the most popular equipment in the industry, it is very important to carry out studies about the effects of voltage flicker on the behavior of the three phase induction motors. Only a few works have been presented on the same topic. One of them has been done in [8–10] using small signal model to evaluate the behavior of the induction motor to regular fluctuations in the terminal voltage. Objective of these papers, is examining the dynamic behavior of induction motors at flicker conditions. Another paper with this topic is [11] which covered the induction motor behavior when the motors are tested by superimposing a second frequency component. Other papers relevant to this article are [12] and [13] where an experimental analysis was applied to evaluate the effects of rectangular voltage amplitude modulations on three phase induction motor behavior. Also reference [14] addresses this problem by emphasizing on several simulations which were performed by using the EMTP/ATP tool. In the work, the effects of voltage fluctuations over efficiency and other characteristics of induction motors in steady state mode of operation are investigated. In all of the cited papers, single cage induction motors have been studied. In fact, it is well-known that the double-cage model of the induction motors must be used to study the behavior of high power motors.

This paper presents the influence of voltage fluctuations on the dynamic behavior of double cage induction motors. Small signal analysis is used to examine the dependency of motor behavior on the frequency of voltage fluctuations and induction motors parameters. Also, this method is implemented for modeling

*Ph.D Student in Engineering Faculty, Shahed University, Tehran, Iran, E-mail: mghaseminejad@shahed.ac.ir.

† Assistance Professor in Engineering Faculty, Shahed University, Tehran, Iran, E-mail: doroudi@shahed.ac.ir (Corresponding Author).

‡ Associate Professor in Electrical Engineering Department, AmirKabar University of Technology, Tehran, Iran, E-mail: hosseinian@aut.ac.ir.

the voltage flicker and induction motors. PSCAD/EMTDC software is also used to validate the model.

The rest of the paper is organized as follows. In section 2 fundamental concepts of small signal modeling of double cage induction motors and voltage fluctuations are presented. Model validation is presented in section 3. In section 4 a quantitative approach is described and finally conclusions are noted in section 5.

II SMALL SIGNAL MODEL

Small signal analysis using linear techniques provides valuable information about the inherent dynamic characteristics of the induction machine. In this model the effects of magnetic saturation, eddy current, and slotting are neglected [15]. On the other hand, disturbances are considered to be small. Therefore the equations that describe the resulting response of the induction machine can be linearized for the purpose of analysis. The voltage fluctuation is a small perturbation that superimposed on the fundamental voltage. This fluctuation is generally considered sufficiently small linearization of system equations. Suitable and small signal model for the analysis of a double-cage induction motor behavior subjected to the regular voltage fluctuations will be presented.

A Double-Cage Induction Motors

Due to its rugged configuration and versatility, the induction motor is the most widely used equipment in industrial environments to perform a set of tasks where mechanical power is needed. Double-cage model of the induction motors should be used to analyze the behavior of high power motors.

Double-cage type induction motors can be modeled with a single-cage model. Deep and narrow rotor bars can be taken into account with this model because they have torque-speed characteristics which are similar to those of a double-cage rotor. Reference [15] illustrates a way that present the equivalent circuit of a double cage induction motor with a single rotor. The equivalent circuit of a double-cage induction motor (i.e. with two rotor bars) is shown in Fig. 11. The model may be represented by an equivalent single rotor circuit as shown in Fig. 22, with slip-dependent rotor parameters:

$$\begin{aligned} R_r(s) &= R_{r0} \frac{m^2 + ms^2 R_1/R_2}{m^2 + s^2} \\ X_r(s) &= X_1 + \frac{R_{r0}(mR_1/R_2)}{m^2 + s^2} \end{aligned} \quad (2)$$

where

$$\begin{aligned} R_{r0} &= \frac{R_1 R_2}{R_1 + R_2} \\ m &= \frac{R_1 + R_2}{X_2} \end{aligned} \quad (3)$$

Based on Fig. 2, Small-signal models in (4) and (7) can be used to analyze the behavior of a double-cage induction motor. Appendix A gives obtaining details of these two equations.

$$\Delta \mathbf{v} = \begin{bmatrix} \mathbf{G}(p) & \Psi_0 \end{bmatrix} \begin{bmatrix} \Delta \Psi \\ \Delta \omega_r \end{bmatrix} \quad (4)$$

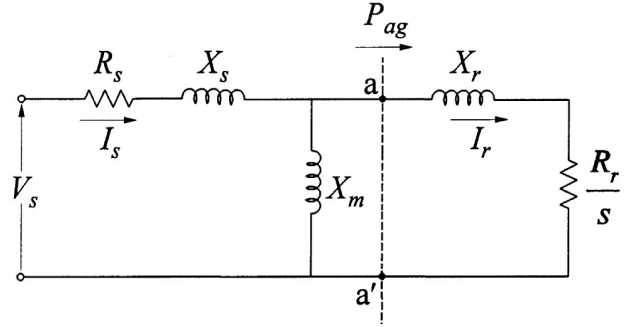


Figure 1: Equivalent circuit of an induction motor with a double-cage rotor.

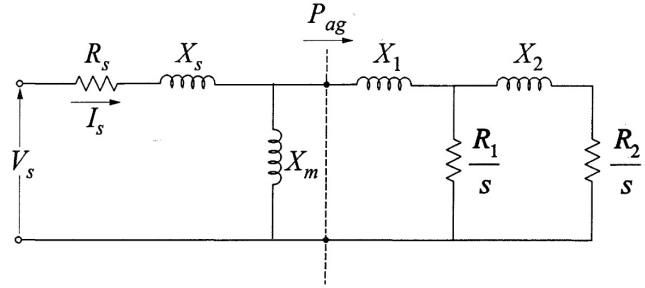


Figure 2: Equivalent single rotor circuit representation of a motor with a double-cage rotor.

in which p is differential operator (d/dt). Also, other vectors and matrix are:

$$\begin{aligned} \Delta \mathbf{v} &= \begin{bmatrix} \Delta v_{ds} & \Delta v_{qs} & \Delta v_{dr} & \Delta v_{qr} \end{bmatrix}^T \\ \Psi_0 &= \begin{bmatrix} \psi_{ds0} & \psi_{qs0} & \psi_{dr0} & \psi_{qr0} \end{bmatrix}^T \\ \Delta \Psi &= \begin{bmatrix} \Delta \psi_{ds} & \Delta \psi_{qs} & \Delta \psi_{dr} & \Delta \psi_{qr} \end{bmatrix}^T \\ \mathbf{G}(p) &= \begin{bmatrix} g_r(p) & -1 & \frac{-R_s L_m}{D} & 0 \\ 1 & g_r(p) & 0 & \frac{-R_s L_m}{D} \\ \frac{-R_r L_m}{D} & 0 & g_s(p) & -s_0 \\ 0 & \frac{-R_r L_m}{D} & s_0 & g_s(p) \end{bmatrix} \end{aligned} \quad (5)$$

where s_0 , $g_r(p)$ and $g_s(p)$ in these relation are:

$$\begin{aligned} s_0 &= \frac{\omega_b - \omega_r}{\omega_b} \\ g_r(p) &= \frac{R_s L_{rr}}{D} + \frac{1}{\omega_b} p \\ g_s(p) &= \frac{R_s L_{ss}}{D} + \frac{1}{\omega_b} p \end{aligned} \quad (6)$$

Moreover, the small signal of torque balance relation is:

$$\Delta T_e - \Delta T_L = 2H\omega_b \frac{d}{dt} \Delta \omega_r \quad (7)$$

Machine variables in Appendix A are expressed as per unit quantities using the following base values [16]:
 V_{base} : Line to neutral peak voltage

I_{base} : Peak line current

Linearized voltage equations and the torque-speed relationship describe the small-signal model of a double-cage three phase induction motor that drives a fan-type load and can be expressed in state space form as $\dot{x} = Ax + Bu$.

B Voltage Fluctuations

In flicker studies it can be assumed that applied voltage is a sinusoidal amplitude modulated signal. In this case sinusoidal superimposed on the fundamental voltage are assumed to be the fluctuating components. With one modulation frequency, the line to neutral voltage of phase “a” is defined as:

$$v_a(t) = V_p [1 + k \sin(\omega_m t)] \cos(\omega_b t) \quad (8)$$

The other phases can be expressed in the same way except which the phase angle of fundamental frequencies in the other two phases should be modified by -120 and $+120$, respectively. The three phase voltages can be transformed into d-q frame to obtain Δv_{ds} , Δv_{qs} . These excursions expressed as per unit quantities are given by:

$$\begin{aligned} \Delta v_{ds} &= 0 \\ \Delta v_{qs} &= k \sin(\omega_m t) \end{aligned} \quad (9)$$

C Model Implementation

Matlab software is used to analyze the small signal model to facilitate calculations. Also a 630 kW double cage induction motor that drives a fan type load is considered for simulation. Motor ratings and its parameters are given in Appendix “B [15]. It is assumed that the induction motor operates at its rated power and the modulating depth (k) is equal to 0.05.

Figs. 3 and 4 show the variations of speed fluctuations and stator current perturbation, respectively for a 10 Hz amplitude modulation frequency. As it can be seen, although the amplitude of speed fluctuations is relatively small, it has a strong influence on the stator current. So, through the simulations carried out, it has been noted that the variations of speed fluctuations can be ignored. But total fluctuating current should be considered. The further conclusion is that voltage fluctuations are reflected in speed oscillations with the same signal modulation frequency.

III MODEL VALIDATION

In order to obtain a broader understanding and small-signal model validation, the large-signal simulations can be carried out. The number of suitable tools for transient analysis is increasing during the last few years. Among these tools we can mention the well known ones as Electro Magnetic Transients Program (EMTP), Electromagnetic Time Domain Transient (PSCAD/EMTDC), MATLAB-SIMULINK, etc. In this work we have used the (PSCAD/EMTDC) program [17], allowing the implementation of the model and the application of power quality disturbances and subsequent analysis of effects.

The integration step of $0.001s$ (account for the delay in rms calculation in PSCAD/EMTDC) is used to validate results of transient simulations in PSCAD/EMTDC. The model consists of a double-cage induction motor (the parameters of the motor

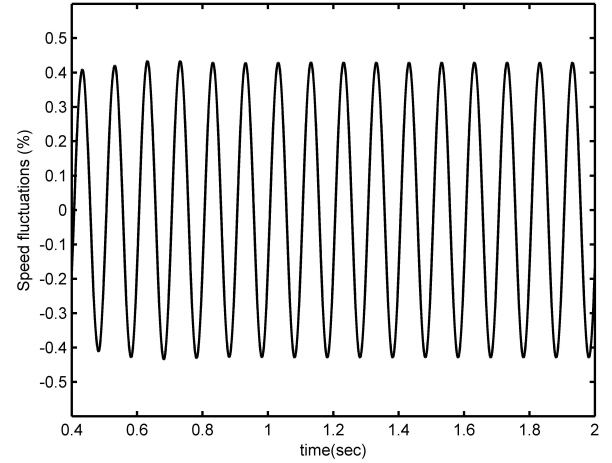


Figure 3: Speed fluctuations for $f_m = 10\text{Hz}$ and $k = 0.05$

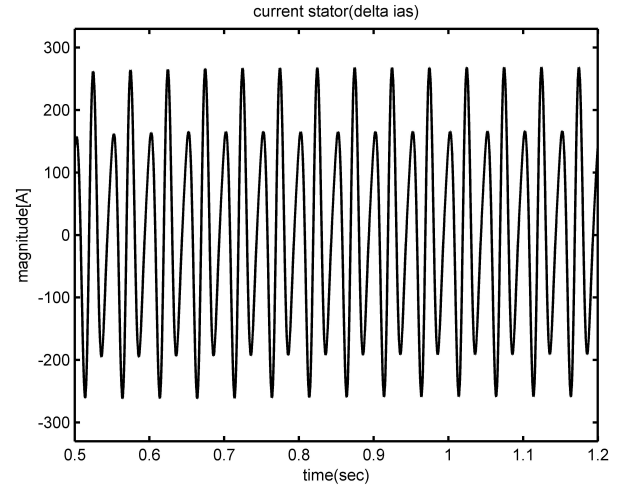


Figure 4: Stator current perturbations for $f_m = 10\text{Hz}$ and $k = 0.05$

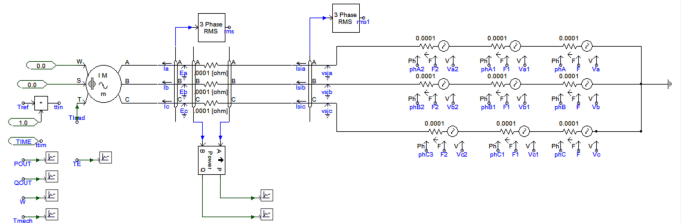
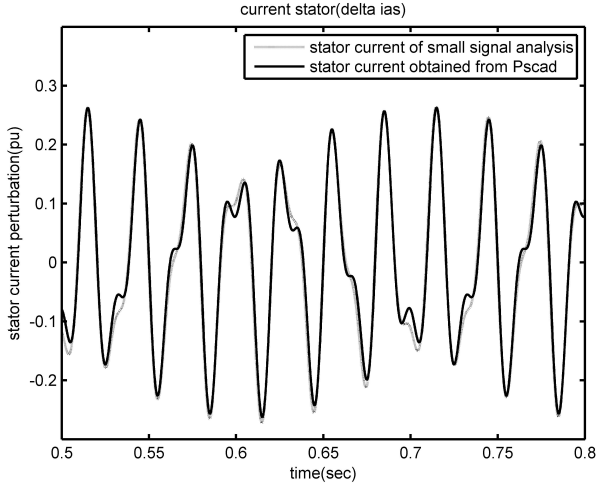


Figure 5: Double cage IM connected to a voltage flicker generator

are given in Appendix “B”) which connected to the PCC bus (as shown in Fig. 5). A flicker generator is also connected to the PCC in order to simulate the voltage fluctuations. Classical transient simulations with full dynamic models of IMs are performed in software to observe the motor transient response under voltage fluctuations conditions. In order to obtain the stator current perturbations from PSCAD simulation, the stator current in the presence of voltage fluctuations subtracted from


 Figure 6: Stator current perturbations for $f_m = 15 \text{ Hz}$ and $k = 0.05$

the stator current in the absence of that signal (normal state). The results have been shown in Fig. 6. In this figure, the stator currents are obtained from the PSCAD simulations and the small signal model and difference of these currents is small.

IV QUANTITATIVE EXPLANATION

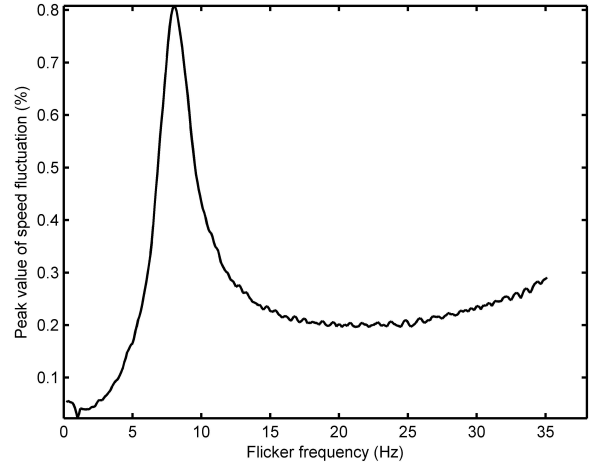
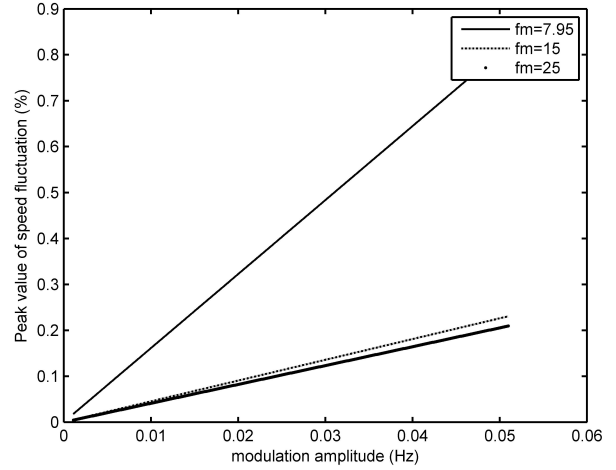
To examine how the induction motor speed changes with respect to frequency of voltage fluctuations, the flicker frequency was changed between 2 to 40 Hz (covering the perceptible flicker frequency range) and speed variations of the induction motor was evaluated. Fig. 7 shows the peak values of speed changes against flicker frequency. The figure indicates that the speed fluctuations are varied with respect to flicker frequency and its maximum peak value occurs at 7.95 Hz.

Fig. 8 shows the motor speed fluctuations against modulating depth in 3 different flicker frequencies. As it can be seen, the most severe speed fluctuations occur for the lower frequency ($f_m = 8 \text{ Hz}$) and it increases with increasing the modulation depth. For $f_m = 15 \text{ Hz}$ and 25 Hz , the speed fluctuations are relatively small and there is a slight increase in speed fluctuations with increasing the modulation depth.

In order to give a quantitative explanation to the speed fluctuations response, the eigenvalues of the system (motor) state matrix are calculated. These values are as follows:

$$\begin{aligned} \lambda_{1,2} &= (-0.0449 \pm j3.1405) \times 10^2 \\ \omega_d &= 3.1405 \times 10^2 \Rightarrow f = 50 \text{ Hz}, \xi = 0.0141 \\ \lambda_{3,4} &= (-0.0608 \pm j0.4959) \times 10^2 \\ \omega_d &= 0.4959 \times 10^2 \Rightarrow f = 7.95, \xi = 0.3214 \\ \lambda_5 &= -0.0791 \times 10^2 \end{aligned} \quad (10)$$

where ξ is damping ratio and ω_d is the undamped natural frequency. As it can be seen, one of the natural frequencies is equal to 7.95 Hz . Applying voltage with this frequency makes maximum speed fluctuations. In fact, when the induction motor is excited by one of the natural frequencies, it reaches to resonance condition and will have the maximum speed fluctuations.


 Figure 7: Peak value of $\Delta\omega_r$ versus flicker frequency

 Figure 8: Peak value of $\Delta\omega_r$ versus modulation amplitude

The participation matrix can be used [9, 15] to find which variable state have a higher influence on the fluctuating mode (corresponding to eigenvalues λ_3 and λ_4). The participation matrix is very useful in small signal analysis. The absolute value of participation factors reveals which parameters are involved in a particular eigenvalue. The participation matrix of the motor is equal to:

$$\mathbf{P} = \begin{matrix} & \lambda_1 & \lambda_2 & \lambda_3 & \lambda_4 & \lambda_5 \\ \begin{bmatrix} 0.5002 & 0.5002 & 0.0001 & 0.0001 & 0.0004 \\ 0.5002 & 0.5002 & 0.0011 & 0.0011 & 0.0000 \\ 0.0002 & 0.0002 & 0.4998 & 0.4998 & 0.0017 \\ 0.0002 & 0.0002 & 0.0038 & 0.0038 & 0.9973 \\ 0.0002 & 0.0002 & 0.5000 & 0.5000 & 0.0013 \end{bmatrix} & \begin{matrix} \Delta\psi_{ds} \\ \Delta\psi_{qs} \\ \Delta\psi_{dr} \\ \Delta\psi_{qr} \\ \Delta\omega \end{matrix} \end{matrix} \quad (11)$$

Above mentioned matrix indicate that $\Delta\psi_{qr}$ and $\Delta\omega$ have high participation in the fluctuating mode corresponding to 7.95 Hz frequency. By analyzing the participation matrix it can be seen that $\Delta\psi_{ds}$, $\Delta\psi_{qs}$ and $\Delta\psi_{dr}$ have a high participation in the fluctuating mode corresponding to 50 Hz frequency and

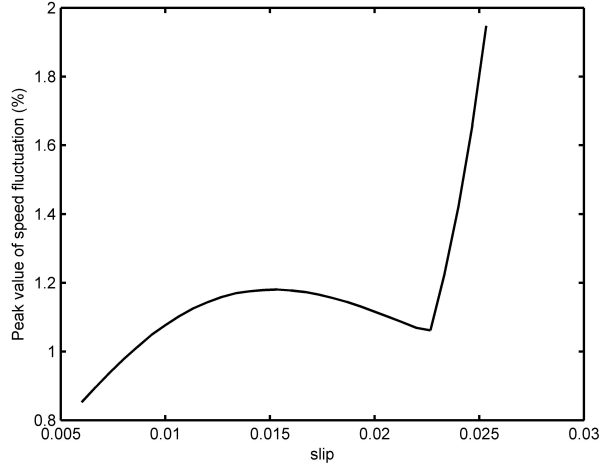


Figure 9: peak value of speed fluctuations versus slip

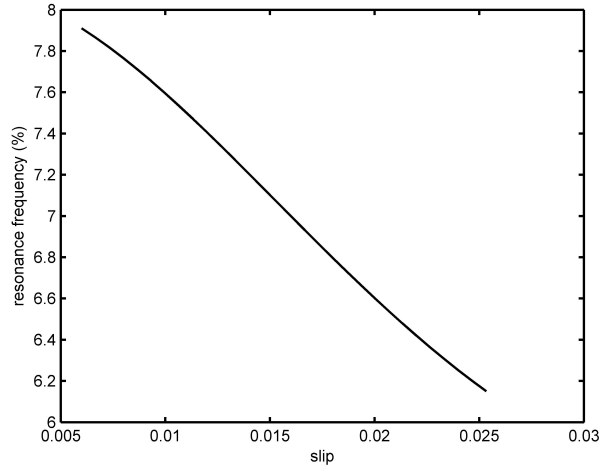


Figure 10: Resonance frequency versus slip

$\Delta p s i_{dr}$ has a higher influence on λ_5 .

As eigenvalues of the state matrix are dependent to machine parameters, it was expected that the slip variations may lead to eigenvalues changes. Hence, the peak value of speed fluctuations changes and occurs at different frequency with slip variations. In order to verify this, the slip value was changed between nominal to pull-out values (covering the perceptible slip range) and speed fluctuations were obtained. Fig. 9 shows the peak value of speed fluctuations with respect to different slip values. Finally, Fig. 10 shows the resonance frequency against slip changes. As it can be seen, the resonance frequency decreases when the slip increases.

V CONCLUSIONS

The increasing level of power quality disturbances has considerable effects on the behavior of electric machines, their loads and also lifetime with the respect to the economic consequences.

Voltage fluctuation is a type of power quality problem which occurs regularly in power systems and its consequences can be very adverse. In this paper, behavior of a double-cage induction motor under regular voltage fluctuations conditions was analyzed by using small signal model. The results show that the induction motor is sensitive to voltage fluctuations within certain amplitude levels and frequencies. The PSCAD/EMTDC tool was applied to verify the performance of the proposed model. Also an eigenvalue based method was applied to give a quantitative explanation to the manner of changing the speed fluctuations.

VI APPENDIX: LINEARIZED MOTOR EQUATIONS

The per unit voltage equations for an induction motor operating at steady state balanced condition can be expressed in synchronously rotating reference frame as follows [16]:

$$\begin{aligned} v_{ds} &= R_s i_{ds} - \psi_{qs} + \frac{1}{\omega_b} \dot{\psi}_{ds} \\ v_{qs} &= R_s i_{qs} + \psi_{ds} + \frac{1}{\omega_b} \dot{\psi}_{qs} \\ v_{dr} &= R_r i_{dr} - s \psi_{qr} + \frac{1}{\omega_b} \dot{\psi}_{dr} \\ v_{qr} &= R_r i_{qr} + s \psi_{dr} + \frac{1}{\omega_b} \dot{\psi}_{qr} \end{aligned} \quad (\text{A-1})$$

The relations between flux linkages and currents are given by:

$$\begin{aligned} i_{ds} &= \frac{1}{D} (L_{rr} \psi_{ds} - L_m \psi_{dr}) \\ i_{dr} &= \frac{1}{D} (-L_m \psi_{ds} + L_{ss} \psi_{dr}) \\ i_{qs} &= \frac{1}{D} (L_{rr} \psi_{qs} - L_m \psi_{qr}) \\ i_{qr} &= \frac{1}{D} (-L_m \psi_{qs} + L_{ss} \psi_{qr}) \end{aligned} \quad (\text{A-2})$$

where:

$$\begin{aligned} L_{ss} &= l_{aa} + L_m \\ L_{rr} &= L_{AA} + L_m \\ D &= L_{ss} L_{rr} - L_m^2 \end{aligned} \quad (\text{A-3})$$

The equations of motion of an induction motor can be described by rotational inertia equation which shows the effect of unbalance between the electromagnetic torque and the mechanical torque of motor as follow:

$$T_e = \frac{2H}{\omega_b} \dot{\omega}_r + T_L \quad (\text{A-4})$$

The air gap and load torques vary with speed. A commonly used expression for the load torque is:

$$\begin{aligned} T_e &= \frac{L_M}{D} (\psi_{dr} \psi_{qs} - \psi_{qr} \psi_{ds}) \\ T_L &= T_0 \omega_r^m \end{aligned} \quad (\text{A-5})$$

From (A-4) and (A-5), we have:

$$\frac{L_M}{D} (\psi_{dr} \psi_{qs} - \psi_{qr} \psi_{ds}) = \frac{2H}{\omega_b} \dot{\omega}_r + T_0 \omega_r^m \quad (\text{A-6})$$

Equations (A-1) to (A-6) can be linearized around an operating point. The linearized of voltage equations are given in (4). Using (A-5) and (A-6), the electromagnetic torque can be obtained as follows ($m = 2$):

$$\Delta T_e - \Delta T_L = 2H\omega_b \frac{d}{dt} \Delta\omega_r \quad (\text{A-7})$$

in which

$$\Delta T_e = \frac{L_M}{D} (\psi_{dr0} \Delta\psi_{qs} + \psi_{qs0} \Delta\psi_{dr} - \psi_{qr0} \Delta\psi_{ds} - \psi_{ds0} \Delta\psi_{qr}) \quad (\text{A-8})$$

Linearized voltage equations and the torque-speed dynamic relationship given by (A-7) and (A-8), respectively, describe the small signal model of an induction machine and can be used to show the dynamic response of motor for small deviations from operating point. Any set of linearly independent system variables which satisfy the equation $\dot{\mathbf{x}} = \mathbf{A}\mathbf{x} + \mathbf{B}\mathbf{u}$ may be used to describe the state of an induction machine. Lets:

$$\mathbf{x} = \begin{bmatrix} \Delta\psi_{ds} & \Delta\psi_{qs} & \Delta\psi_{dr} & \Delta\psi_{qr} & \Delta\omega_r \end{bmatrix}^T \quad (\text{A-9})$$

$$\mathbf{u} = \begin{bmatrix} \Delta v_{ds} & \Delta v_{qs} & \Delta v_{dr} & \Delta v_{qr} \end{bmatrix}^T$$

Then we have:

$$\mathbf{A} = \omega_b \begin{bmatrix} \frac{-R_s L_{rr}}{D} & 1 & \frac{R_s L_m}{D} & 0 & 0 \\ -1 & \frac{-R_s L_{rr}}{D} & 0 & \frac{R_s L_m}{D} & 0 \\ \frac{R_r L_m}{D} & 0 & \frac{-R_r L_m}{D} & s_0 & -\psi_{qro} \\ 0 & R_r L_m & -s_0 D & -R_r L_{ss} & \psi_{dro} \\ -k\psi_{qro} & k\psi_{dro} & k\psi_{qso} & -k\psi_{dso} & -\frac{T_0 \omega_{ro}}{H\omega_b} \end{bmatrix} \quad (\text{A-10})$$

and

$$\mathbf{B} = \begin{bmatrix} 1 & 0 & 0 & 0 & 0 \\ 0 & 1 & 0 & 0 & 0 \\ 0 & 0 & 1 & 0 & 0 \\ 0 & 0 & 0 & 1 & 0 \end{bmatrix}^T \quad (\text{A-11})$$

$$k = \frac{L_m}{2H\omega_b}$$

These equations form a minimal set of dynamic variables along with the inputs to the system and provide a complete description of the induction motor behavior. A complete overview of induction machine behavior when the machine experiences voltage fluctuations is presented and the main advantage of small signal modeling of induction machine is illustrated. Finally, the parameters of the proposed system and the main symbols of the paper are shown in Tables A-1 and A-2, respectively.

REFERENCES

- [1] R. C. Dugan and *et al.*, "Electrical Power systems Quality," 2nd ed., McGraw-Hill, 2004.
- [2] J. A. Arrillaga, N. R. Watson and S. P. Chen, "Power System Quality Assessment," New York, John Wiley & Son, 2000.
- [3] *IEEE Standard Dictionary of Electrical and Electronics Terms*, Std. 100, IEEE, 1984.

Table A-1: Specification of Boost Converter.

Description	Parameter	Value
Rated voltage	V	400 volts
Rated power	P	630 kw
Rated current	I	1400 A
Rated speed	n_r	1492 rpm
Stator resistance	R_s	0.000647 Ω
Inner cage rotor resistance	R_2	0.0253 Ω
Outer cage rotor resistance	R_1	0.00129 Ω
Inner cage leakage inductance	X_{lr1}	0.0303 Ω
Outer cage leakage inductance	X_{lr2}	0.0168 Ω
Mutual inductance	X_m	0.673 Ω
Stator leakage inductance	X_{ls}	0.0168 Ω
Momentum of inertia	j	14 $kg^2.s$

Table A-2: List of Main Symbols.

Symbol	Quantity
f_b	Fundamental frequency
V_b	Line to neutral peak voltage
v_d, v_q	dq axes voltages
i_d, i_q	qd axes currents
ψ_d, ψ_q	dq axes flux linkages
R_s	Stator resistance
L_{ls}	Stator leakage inductance
R_r	Rotor resistance
L_{lr}	Rotor leakage inductance
L_m	Mutual inductance
H	Inertia constant
ω_b	Base angular frequency
ω_r	Rotor angular speed
f_b	Modulation (flicker) frequency
k	Modulation depth
T_L	Load torque
s subscript	Stator variables
r subscript	Rotor variables
o subscript	Steady state values

- [4] J. Jatskevich, O. Wasynczuk and L. Conrad, "A method of evaluating flicker and flicker reduction strategies in power systems," IEEE Trans. on Power Delivery, vol. 13, no. 4, pp.1481-1487, Oct. 1998.
- [5] W. N. Chang, C. J. Wu and S. S. Yen, "A flexible voltage flicker teaching facility for electric power quality education," IEEE Trans. Power Systems, vol. 13, no. 1, pp. 27-33, Feb. 1998.
- [6] M. Bollen and I. Y. H. Gu, "Signal Processing of Power Quality Disturbance," New York, IEEE Press, John Wiley & Sons, 2006.
- [7] M. M. Morcos and J. C. Gome, "Flicker sources and mitigation," IEEE Power Engineering Review, vol. 22, no. 11, November 2002.
- [8] S. Tennakoon, S. Perera and D. Robinson, "Flicker attenuation-Part I: Response of three phase induction motors to regular voltage fluctuations," IEEE Trans. Power Delivery, vol. 23, no. 2, pp. 1207-1214, April 2008.
- [9] M. Ghaseminezhad, A. Doroudi and S. H. Hosseini, "Evaluation of the Effects of the Regular Voltage Fluctuations on Induction Motors Behavior," presented at the 24th International Power System Conference, Tehran, Iran, 2009.
- [10] M. GhasemiNezhad, A. Doroudi and S. H. Hosseini, "A Novel Equivalent Circuit for Induction Motor under Voltage Fluctuation Conditions," Amirkabir Journal of Science & Technology/Electrical & Electronics Engineering, vol. 44, no.1, pp. 53-61, Spring 2012.

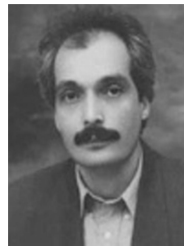
- [11] C. Grantham, H. Tabatabaei-Yazdi and M. F. Rahman, "Efficiency evaluation of three phase induction motors by synthetic loading," presented at the Proc. 1997 Power Electronics and Drive Systems Conf., Tehran, Iran, 1997.
- [12] G. Bucci and *et al.*, "Effect of the voltage amplitude fluctuations on induction motors," presented at the Symposium on Power Electronics, Electrical Derives, Automation and Motion, SPEEDAM, Capri, Italy, June 2004.
- [13] G. Bucci, F. Ciancetta, A. Ometto and N. Rotondale "The evaluation of the effects of the voltage amplitude modulations on induction motors," presented at the Power Tech, St. Petersburg, Russia, 2005.
- [14] J. Baptista and *et al.*, "Induction motor response to periodical voltage fluctuation," presented at the Proc. 2010 Electrical Machines (ICEM), Rome, Italy, Sept. 2010.
- [15] P. Kundur, "Power System Stability and Control," McGraw-Hill, 1994.
- [16] P. C. Krause, O. Wasynczuk and S. D. Sudhoff "Analysis of Electric Machinery," 2nd ed., New York, Wiley, 2002.
- [17] B. M. Winnipeg, "PSCAD 4.1.1 On-Line Help File," Manitoba HVDC Research Centre, Manitoba, Canada, 2004.



Morteza GhasemiNezhad was born in Bardsir, Kerman, Iran, in 1985. He received the B.Sc. degree from the Electrical Eng. Dept. of Shahid bahonar University, Kerman, Iran, in 2007 and the M.Sc. degree in electrical engineering from Shahed University, Tehran, Iran, in 2010. He is a Ph.D. student in the Electrical Engineering Department, Shahed University, Tehran, Iran. His especial fields of interest include power systems dynamics and Power Quality.



Aref Doroudi was born in 1968 in Tehran, Iran. He received the B.Sc. degree from the Electrical Eng. Dept. of Amirkabir University of technology, Tehran, Iran, in 1992 and the M.Sc. degree in electrical engineering from Tabriz University, Tabriz, Iran, in 1994 and PhD degree in Electrical Engineering Dept, of Amirkabir University of technology, Tehran, Iran, in 2000. At the present, he is the assistant Professor of Electrical engineering Department in Shahed University, Tehran, Iran. His especial fields of interest include Power Quality, Electric Machines Design and power systems dynamic.



Seyed Hossein Hosseinian was born in 1961 in Iran. He received both the B.Sc. and M.Sc. degrees from the Electrical Eng. Dept. of Amirkabir University of technology, Iran, in 1985, and 1988, respectively, and PhD degree in Electrical Engineering Dept, university of Newcastle England, 1996. At the present, he is the associated Professor of Electrical engineering Department in Amirkabir University of technology (AUT). His especial fields of interest include transient in power systems, Power Quality, Restructuring and Deregulation in power systems. He is the author of four books in the field of power systems. He is also the author and the coauthor of over one hundred technical papers.